放射光の医学利用
と
放射線治療

篠原邦夫
早稲田大学理工学術院
総合研究所理工学研究所

Spring-8利用推進協議会
第6回安全安心のための分析評価研究会
2012.4.27. 於 東京理科大学

放射光の医学利用と放射線治療

１．放射光の特徴
２．医学利用研究の概要
３．放射線治療に関する基礎研究の概要
４．MRT研究の背景
５．正常組織への影響
６．動物実験における延命効果
７．作用機構について
７．線量分布のエネルギー依存性
８．今後の課題

医・生物学利用における放射光の特徴

高輝度→顕微観察

→位相情報

高強度→単色X線源

光子活性化療法

→短時間露光

微小ビーム

放射線療法

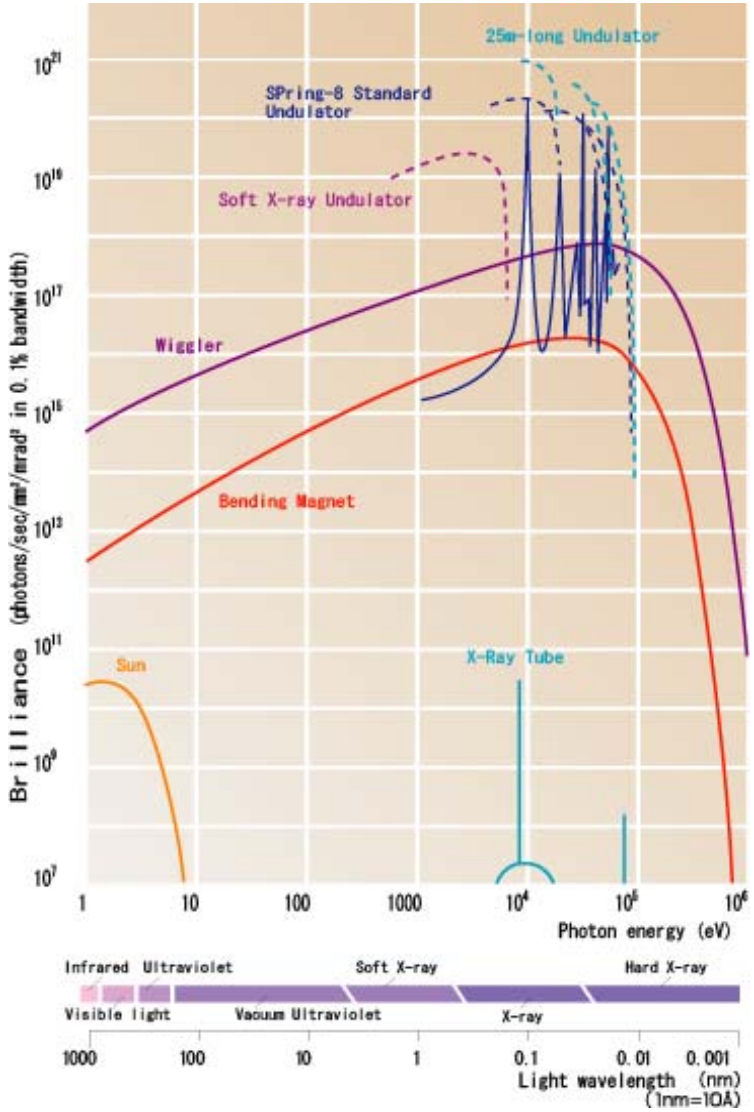

SPring-8のポスター

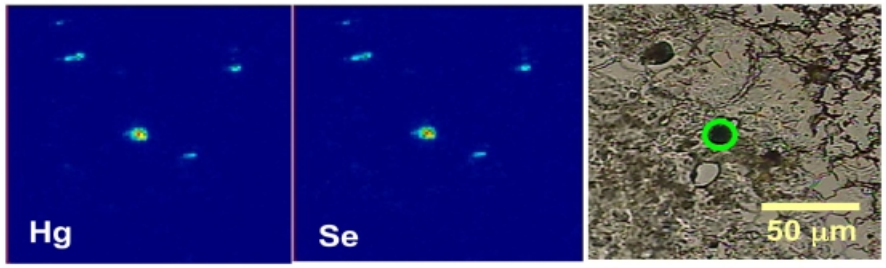

肝臓のマイクロ-
XRFイメージング

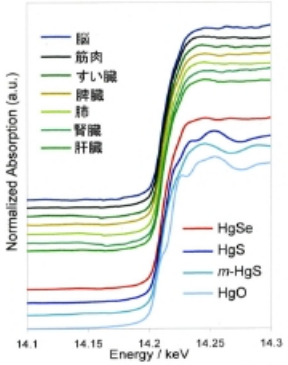

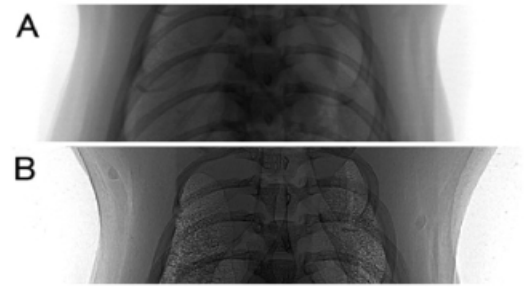

蛍光X線分析

細胞(組織)内
微量元素分析
マッピング

蛍光X線放出

XAFS（X線吸収微細構造）

細胞(組織)内
原子分子分析
マッピング

光電子分光

生体分子の解析
光電子顕微鏡

光電子放出

位相変化

透過X線

イメージング

個体・細胞・組織
構造観察
(含顕微・造影)

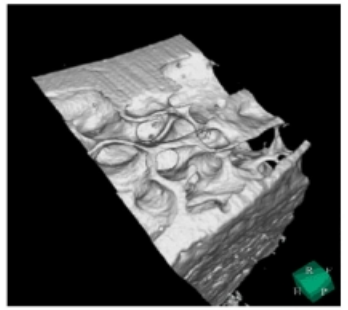

吸収

物質

照射効果

入射X線

生物作用
治療の基礎

回折・散乱X線

結晶構造解析
小角散乱
回折顕微法

回折・散乱

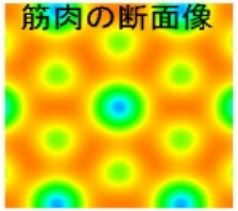

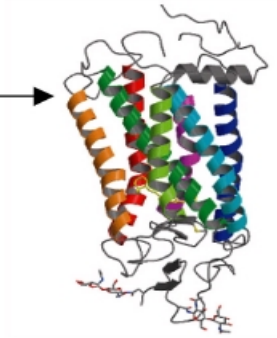

ウシ・ロドプシン結晶構造の模式図

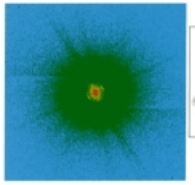

図1.大腸菌試料からのコヒーレントX線散乱パターン

図2. 図1の散乱パターンから再構成された実空間像(25 nm分解能)

放射光と医・生物学

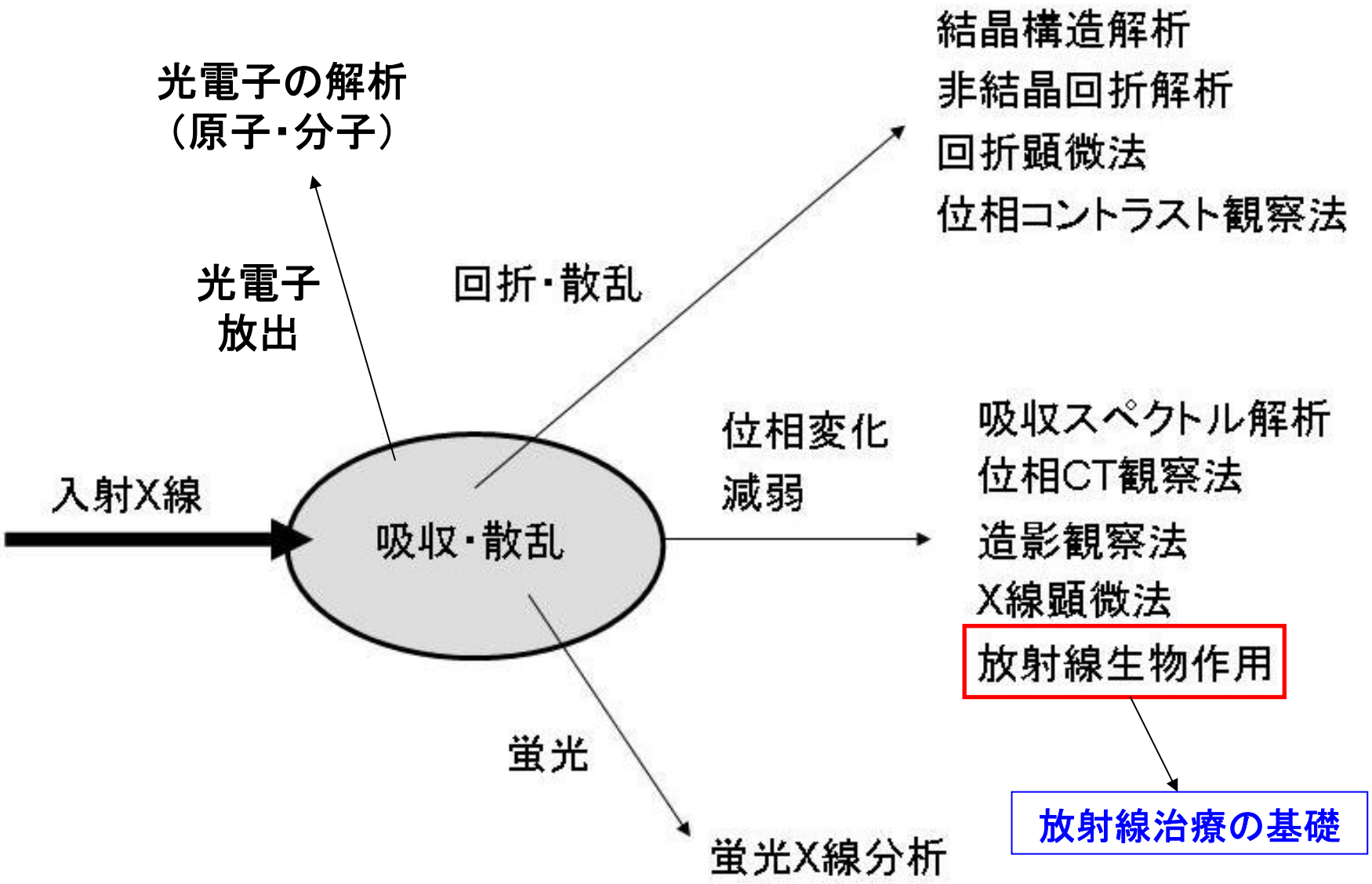
光電子の解析
（原子・分子）
光電子
放出
回折・散乱
結晶構造解析
非結晶回折解析
回折顕微法
位相コントラスト観察法
入射X線
吸収・散乱
位相変化
減弱
吸収スペクトル解析
位相CT観察法
造影観察法
X線顕微法
放射線生物作用
放射線治療の基礎
蛍光
蛍光X線分析

放射光による

放射線治療の基礎研究

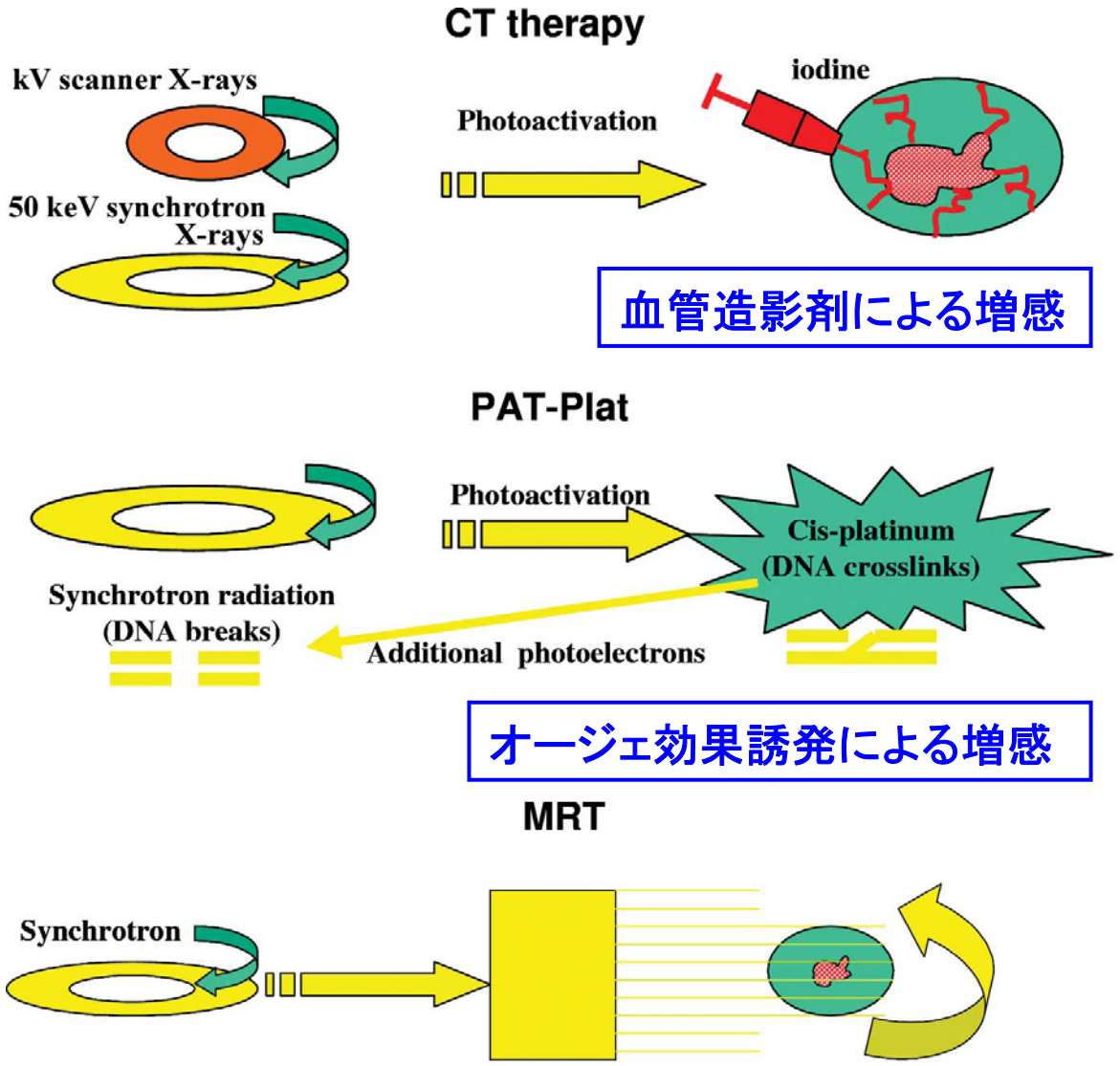

Bencokova et al, J. Synchrotron Radiat. 15, 74, 2008

放射線治療の基礎研究

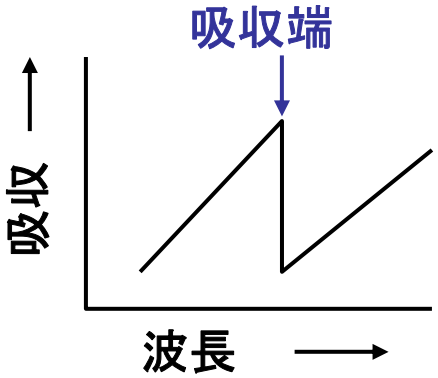

- 光子活性化療法　⇛　X線エネルギー依存性

  DNAに結合する原子とそのK吸収端付近の単色X線照射を組み合わせて、致死増感効果を誘導する。(細胞毒性が粒子線並みのオージェ効果の誘発)･･･オージェ効果の寄与は数割程度の致死増感と見積もられた。

- 微小平板ビーム治療　⇛　超高線量率照射

  ラットの脳腫瘍に、数十μm幅のビームを数百μm間隔にして照射すると、1回線量625 Gyで、皮膚の放射線障害は回復し、延命効果があった。

オージェ効果を利用する

光子活性化療法とは

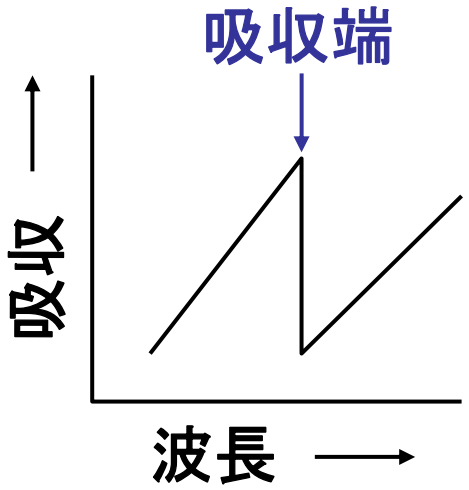

1．腫瘍集積性の元素を癌に取り込ませて、X線吸収における選択性をつける。

2．選択的に吸収する波長のX線を照射する。

3．その元素のX線吸収後に二次的に誘発されるオージェ効果の細胞毒性を利用する。

オージェ効果の細胞致死作用

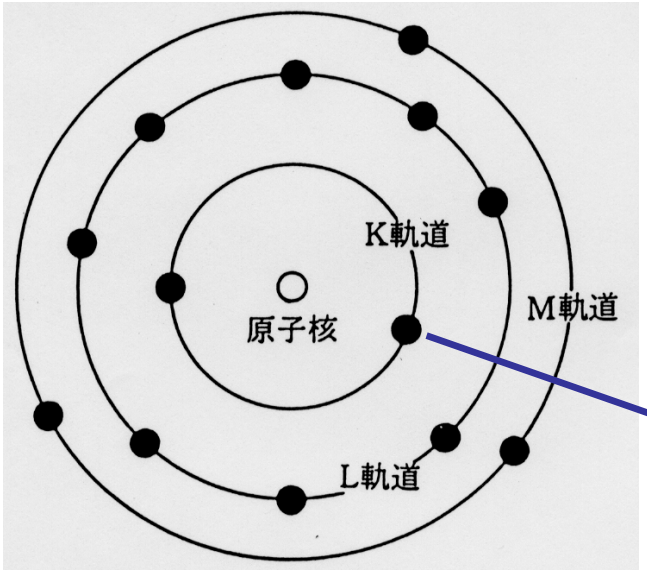

電離

e^-

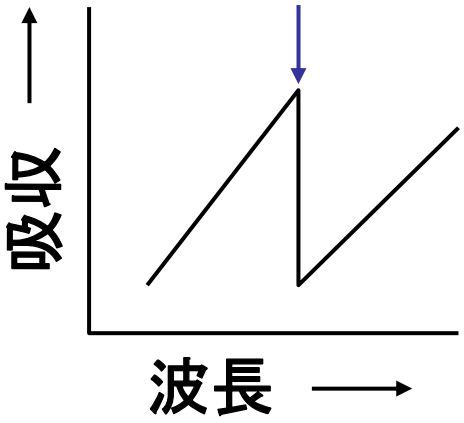

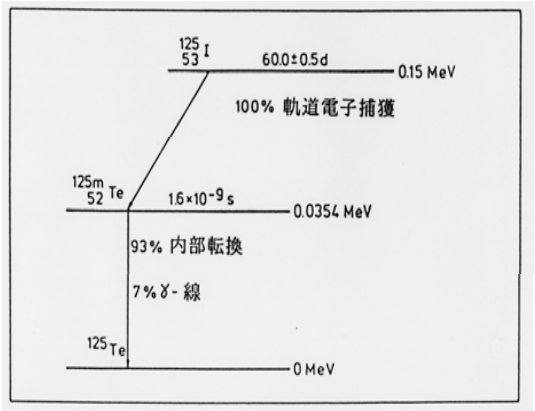

^{125}Iの壊変様式

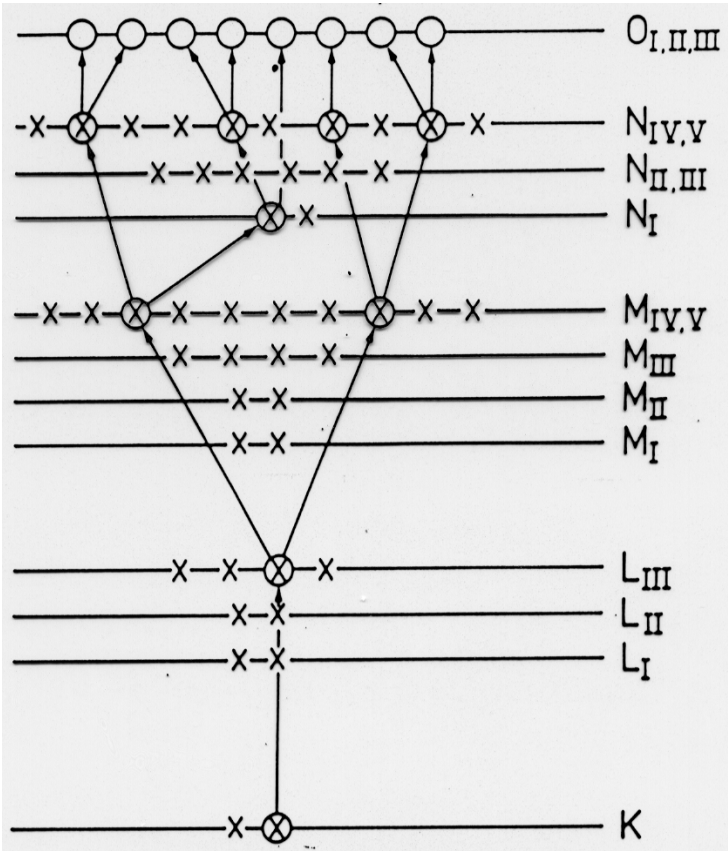

（XeのK殻に空きができた場合）

Halpern A, in Uses of Synchrotron Radiation in Biology (Ed. by Stuhrmann HB), pp.255-283, 1982

オージェ効果（オージェ電子群）の細胞致死作用の特徴

^{125}IUdRのDNA取り込み実験より

1. 細胞致死作用が非常に大きい
2. 傷害の局在性が高い（主に1.5-2nm以内）
3. 酸素効果が小さい（OER≦1.4）
4. LETが5MeVのα粒子（≧100keV/μm）相当
5. 主に直接作用（DMSOで防護されにくい）
6. 細胞周期依存性が低い

光子活性化療法の理論

$$D_E = F\{S \cdot D + C \cdot D\,(S \cdot \Phi_{TOT} + G \cdot \Phi_e \cdot O)\} \quad (1)$$

where

D	=	absorbed dose to normal cells in rd,
D_E	=	enhanced dose,
S	=	radiation sensitization due to low LET radiation,
C	=	cross section ratio, described above,
Φ_{TOT}, Φ_e	=	fraction of total photoelectric effect energy absorbed locally (Φ_{TOT}) and of total energy released as primary, Auger, and Coster-Kronig electrons (Φ_e),
G	=	geometrical advantage due to Auger effect in DNA,
F	=	high LET enhancement due to recovery of normal tissue from effects of low LET radiation, and
O	=	Oxygen gain factor (OGF) of Auger electrons, where OGF is the ratio of OER (oxygen enhancement ratio) for standard 250 kVp X-rays to the test system OER.

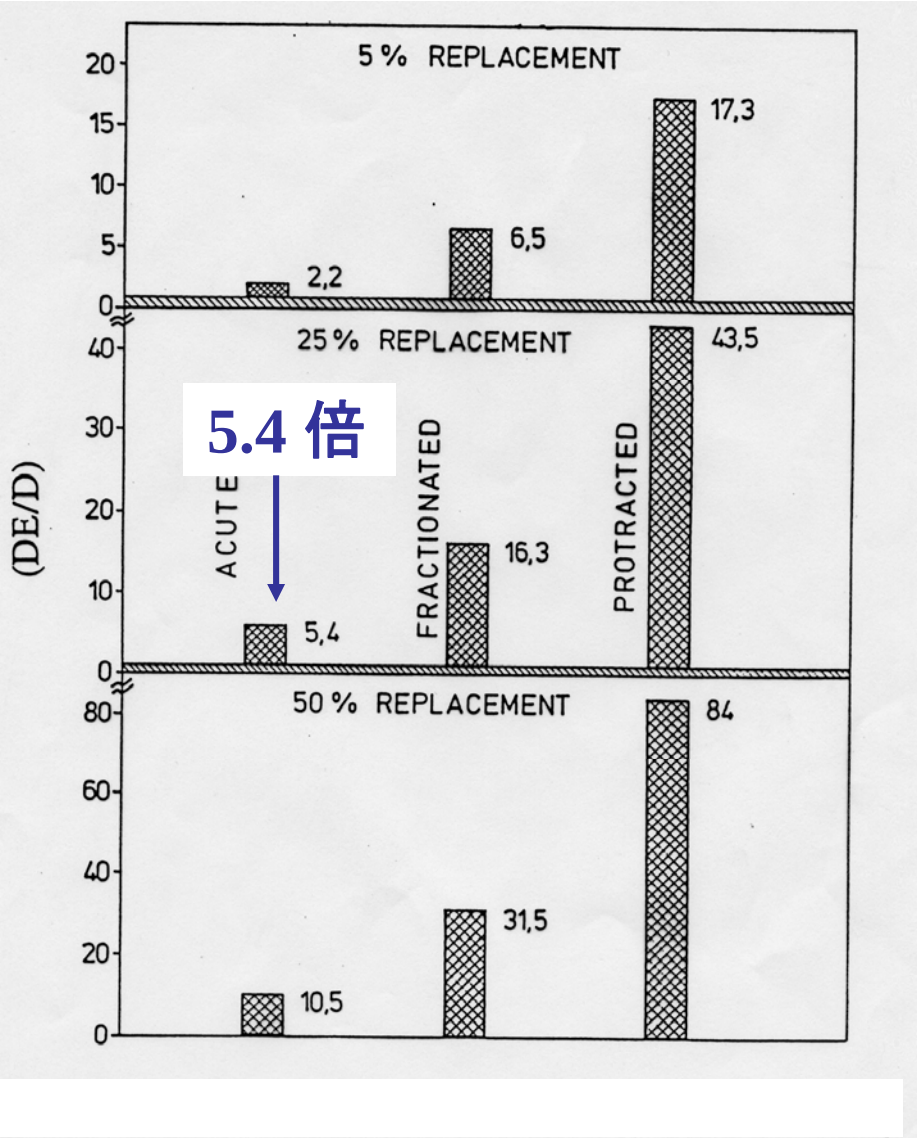

D_E/D: 増感率

Fairchild and Bond, Strahlentherapie 160, 758, 1984

5-iododeoxyuridine (IUdR)

I-K_{ab} : 0.0374 nm (33.17 keV)

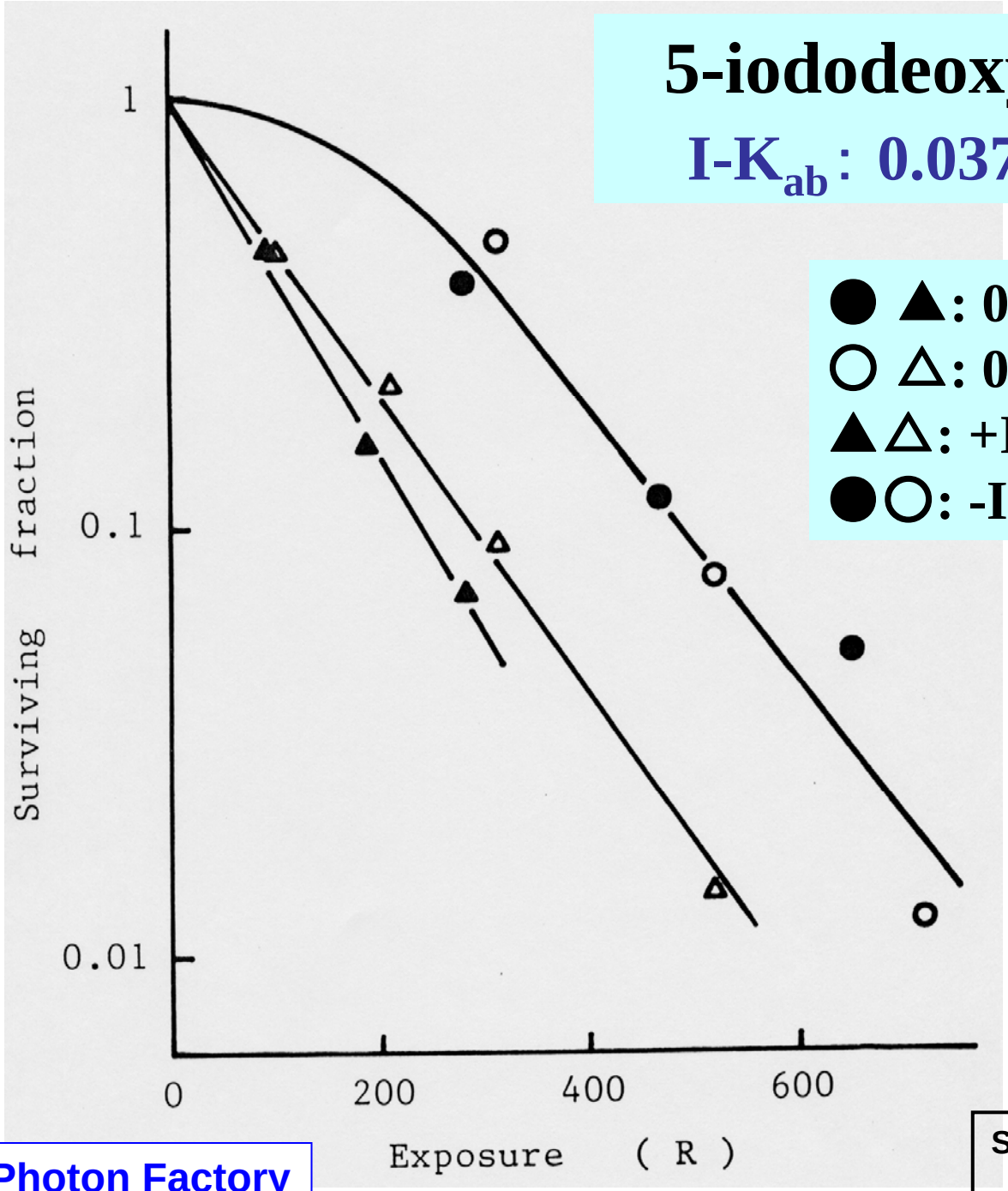

● ▲: 0.037 nm (33.5 keV)
○ △: 0.038 nm
▲△: +IUdR（置換率：20% ）
●○: -IUdR

	D_E/D
実験値*	2.05
理論値	4.61

*10%生存率で比較

Photon Factory

Shinohara et al, Photon Factory Activity Report 1984/1985, 225, 1986

D* = 0.27D（間接作用が73%）

$$D_E = F\{S \cdot D + C \cdot D\,(S \cdot \Phi_{TOT} + G \cdot \Phi_e \cdot O)\} \quad (1)$$

Fairchild and Bond（1984）の式

where

D = absorbed dose to normal cells in rd,
D_E = enhanced dose,
S = radiation sensitization due to low LET radiation, **= 1.8**
C = cross section ratio, described above,
Φ_{TOT}, Φ_e = fraction of total photoelectric effect energy absorbed locally (Φ_{TOT}) and of total energy released as primary Auger, and Coster-Kronig electrons
G = geometrical advantage due to
F = high LET enhancement due
from effects of low LET radia
O = Oxygen gain factor (OGF) of
is the ratio of OER (oxygen e
ard 250 kVp X-rays to the test system OER.

	D_E/D
実験値*	2.05
理論値	4.61
修正値	2.56

Shinohara et al, Photon Factory Activity Report 1986, 278, 1987

710 NEWS AND VIEWS NATURE VOL. 336 22/29 DECEMBER 1988

Cancer

Therapy by photon activation?

John Humm

EXPERIENCE with conventional radiotherapy has shown that to treat cancer successfully, the maximum dose possible must be delivered to the tumour — typically 50–80 Gy (5,000–8,000 rad) — compatible with the tolerances of the normal sensitive body tissues. A new approach to radiotherapy proposed by R. L. Mills *et al.* elsewhere in this issue (*Nature* 336, 787–789; 1988), uses a Mössbauer resonance absorption technique selectively to deliver sterilizing doses to tumour cells, at the expense of only about 10^{-5} Gy to the normal tissues. There is impressive tumour ablation in tumour-bearing mice after minute radiation doses, and the authors allude to the implications for this kind of therapy in man: significant regression and maybe even cure at doses less than received by a chest X-ray.

The Mössbauer effect arises with particular radionuclide γ-transitions when the source is tightly bound within a crystal lattice. Under these conditions, the crystal as a whole can recoil, but if the recoil energy is insufficient to excite the lowest quantized phonon level of the crystal, the emission can be totally without recoil and the full emission energy is carried by the γ-photon. When this happens, a resonant reabsorption of the source emission line by an adjacent atom in the de-excited state becomes highly probable because of the exact overlap between the parent emission and the daughter absorption bandwidths. This very high-absorption cross-section, Mills and his colleagues propose, could be exploited for a novel kind of radiotherapy.

Selective absorption

Conventional radiotherapy uses high-energy γ-photons produced either by a ^{60}Co source machine or by high-energy accelerators such as a LINAC. The primary mode of energy deposition by such high-energy photons is Compton scattering, the cross-section of which varies only slightly between the different tissue constituents. If it were possible to obtain a selective absorption of radiation in some element which could be preferentially incorporated into tumour tissue via a cancer-localizing drug, then the basis of a therapy might be established. There are two potential highly selective mechanisms of photon absorption: the photoelectric effect and the Mössbauer effect.

The photoelectric effect becomes the dominant photon-interaction process in tissue at energies less than 60 keV. Because the photoelectric cross-section increases with atomic number Z as Z^4, if a high-Z element such as iodine could be readily and specifically incorporated into tumour tissue and then exposed to photons of energy just above the binding energy of the innermost orbital of iodine, a selective absorption in iodine might be induced when the differential cross-section of iodine compared to tissue peaks sharply. The photoelectric cross-section of iodine just above the K-shell binding energy (33.2 keV) is 38.4 cm^2 per g versus 0.15 cm^2 per g for tissue at this energy, a gain of about 250. But before too much jubilation, the predominant constituent by weight of normal tissue, oxygen, is probably at least 1,000 fold in excess of the level of iodine achievable in the cell nucleus.

But what if a high-Z element could be specifically incorporated into the DNA of the target cell? A photoelectric interaction, which induces an inner-shell electron vacancy within an atom, initiates an electronic de-excitation process involving a cascade of inner-shell transitions through the atom, the result of which is the emission of characteristic X-rays and, more important, a shower of low-energy Auger electrons. These Auger electrons, the result of many outer-shell non-radiative transitions, predominantly have ranges of only a few nanometres. The radionuclide ^{125}I, which induces inner-shell vacancies by the decay process, if appended to the DNA, the prime target for cell inactivation, can blow the DNA to pieces near the site of decay (Martin, R. F. & Haseltine, W. A. *Science* 213, 896–898; 1981). Iodine can be selectively incorporated into the DNA of rapidly dividing tissue like tumour cells by the substitution of thymidine by an analogue iododeoxyuridine. Unfortunately, normal tissues such as the gastro-intestinal tract and bone marrow also have a rapid turnover. Proponents of photoactivation therapy therefore argue that the advantage of induced cascades by a cold analogue over a radiolabelled analogue is the ability to spare normal sensitive tissues by the beam geometry.

The excitement over the alleged potential of this technique has stimulated many groups to test its feasibility using cell cultures. The most recent study, by the group of Professor T. Ito at Tokyo University, uses Photon Factory, a synchrotron producing a tunable intense monochromatic beam of photons. The group measured the magnitude of Auger-enhanced cell killing in a mammalian cell culture with up to 20 per cent substitution of thymidine with iododeoxyuridine irradiated just above the K-edge of iodine Shinohara, K. *et al. Photon Factory Activity Report* 4, 278; 1987). The effects they observed are disappointingly small: they obtain an enhancement of 1.25 in traversing the K-edge of iodine, whereas that in uniodinated cells (illustrating the degree by which the DNA is sensitized by the substituted thymidine analogue) is 2.05.

Therapeutic implications

The failure of these studies to obtain sizable enhancements that could have therapeutic implications raises the following dilemma. On the one hand, the incorporated material must be sufficient to present an interaction cross-section large enough to outweigh the effect of the dose from the secondary electron flux produced by photoelectric interactions in all the elements normally present in tissue. On the other, it must not be so high as to impair severely the fidelity of the DNA.

The work by Mills *et al.* reported in this issue at first sight offers new hope for photoactivation therapy, the highest ever measured Mössbauer cross-section is with the 14.4-keV excitation state of ^{57}Fe (27,139 cm^2 per g), about 15,000 times greater than tissue at this energy. The approach of Mills *et al.* is to use a ^{57}Fe–bleomycin conjugate. Bleomycin is a tumoricidal agent which intercalates between the strands of DNA. Mills *et al.* irradiated the tumour with a moving ^{57}Co source incorporated in a rhodium matrix. The source motion produces a Doppler shift in the γ-emission frequency and enables any mismatch between source and target environment to be retuned for resonance absorption. An incoming photon which interacts with an ^{57}Fe atom excites it to the 14.4-keV level from which it instantaneously (in about 10 ns) reverts to the ground state by internal conversion in 91 per cent of cases. Internal conversion produces an inner-shell electron vacancy and thus an Auger cascade, which could result in a high radiotoxicity for photon interactions in the ^{57}Fe in the DNA.

This study is a highly original piece of work and warrants further investigation. But I cannot help being sceptical about claims of considerable tumour regression at doses as low as 10^{-5} Gy. If the results are so great with such an insignificant dose, why not use a bigger source, deliver 0.01 Gy and cure the animals altogether? My reservations concerning the paper hinge on three points. First, a decisive control is needed, that is, moving the source at a velocity which intentionally corresponds to a Doppler shift well off the Mössbauer resonance peak. Second, the level of drug administered intra-tumorally, although well below toxicity levels for the animal, would cause considerable toxicity to the tumour, certainly if the levels of DNA intercalation reported of one drug molecule per six DNA base pairs are to be believed. On the other hand, if the drug

NEWS AND VIEWS
(NATURE, 336, 710, 1988)

Mössbauer cross-section

→ 原子核の励起

		D_E/D
軌道電子	実験値	2.05
	理論値	2.56
核の励起	理論値	28.5

Shinohara, K.

（参考）最近の報文

＊S. J. Karnas et al:

Optimal photon energies for IUdR K-edge radiosensitization with filtered X-ray and radioisotope sources. Phys. Med. Biol. 44 (1999) 2537.

＊M.-C. Biston et al:

Cure of Fisher rats bearing radioresistant F98 glioma treated with cis-platinum and irradiated with monochromatic synchrotron X-rays. Cancer Res. 64 (2004) 2317.

＊S. Corde et al:

Synchrotron radiation-based experimental determination of the optimal energy for cell radiotoxicity enhancement following photoelectric effect on stable iodinated compounds. Br. J. Cancer (2004) 544.

微小平板ビーム放射線治療
MRT (Micro-planarbeam Radiation Therapy)

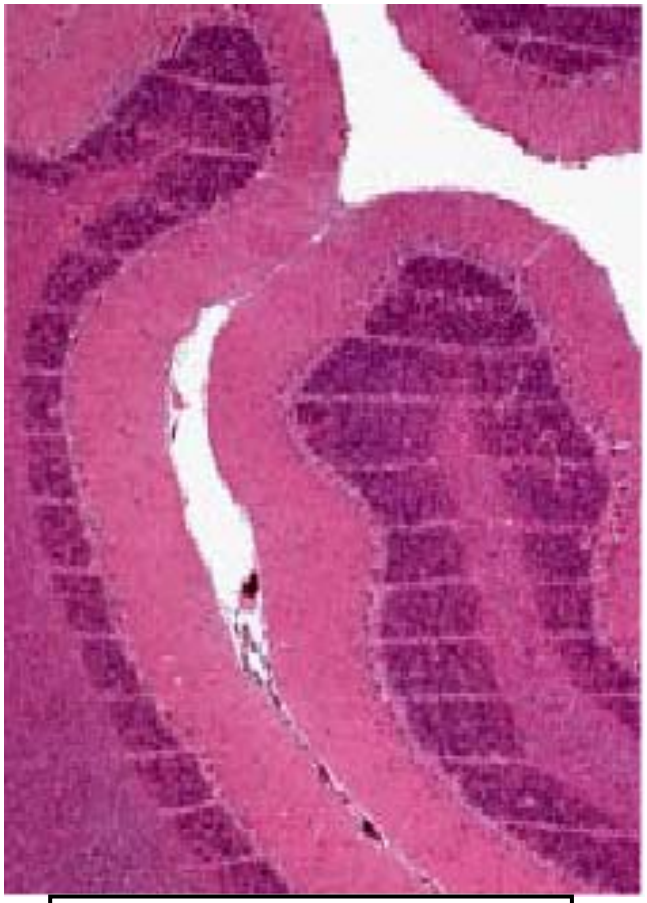

Laissue et al, Proc. SPIE 4508, 65, 2001

方法

スリット状の放射光を照射する

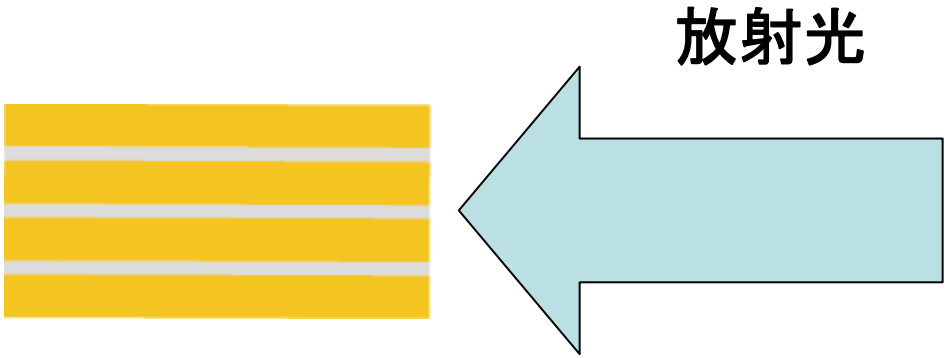

特徴

ラットの脳腫瘍に、数十μm幅のビームを数百μm 間隔にして照射すると、1回線量625 Gyで、皮膚の放射線障害は回復し、延命効果があった。

背景（粒子線の影響）

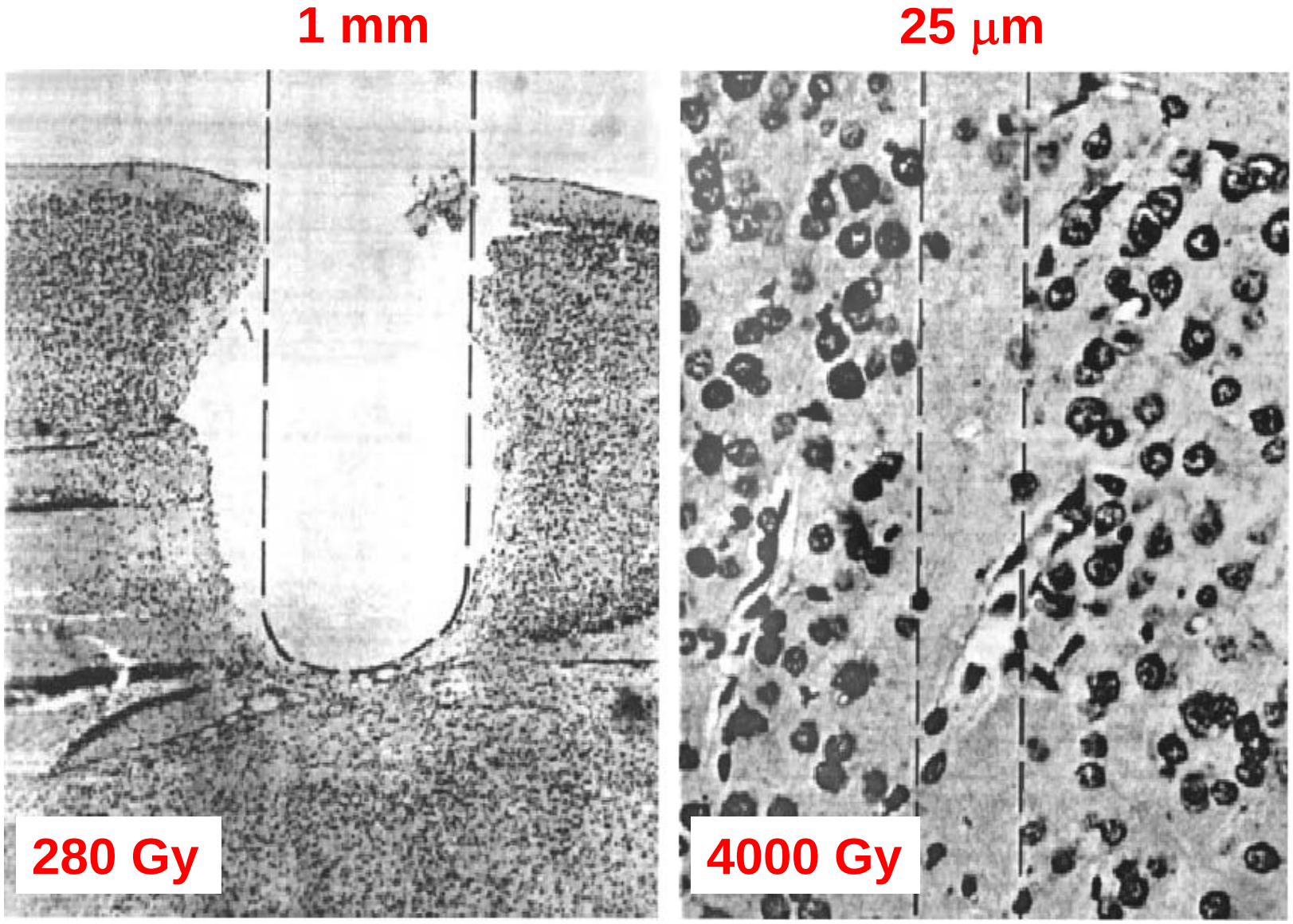

Zeman et al, Radiat. Res. 15, 496, 1961

概要

1961 Zeman et al：粒子線マイクロビームの影響
1963 Straile and Chase： X線マイクロビームによる検討
1992 Slatkin et al：放射光マイクロビーム放射線治療の提案
1995 Slatkin et al：放射光マイクロビーム放射線の正常組織(rat頭部）への照射

（正常組織への影響）

1999 Laissue et al ：suckling rats
2000 Schweizer (Laissue) et al ：Drosophila melanogaster
2001 Dilmanian et al ：duck embryos
2001 Laissue et al ：piglets
2003 Zhong (Dilmanian) et al ：rat skin

（制癌作用）

1998 Laissue et al ：rat 9L gliosarcoma
2002 Dilmanian et al ：rat 9L gliosarcoma
2003 Dilmanian et al ：murine EMT-6 carcinoma
2006 Smilowitz (Laissue) et al ：rat 9L gliosarcoma
2006 Miura (Laissue) et al ：murine SCCVII squamous cell carcinoma

Table 1. Dose–effect studies on the brains of microbeam-irradiated rats

Exp.	Beam cross section: Width	Beam cross section: Height	Rat no.	Approximate entrance absorbed dose, Gy	No. of irradiated slices	Microplanar beam thickness, μm	Intervals between slices, on center, μm	Brain lesions in histological sections
MRT 2	20 μm	4 mm	2	5,000	3	20 ± 2	200	Loss of nuclei*
			3	5,000	3	20 ± 2	200	Loss of nuclei
			5	10,000	3	20 ± 2	200	Loss of nuclei
			6	10,000	3	20 ± 2	200	Loss of nuclei
			7	2,500	3	20 ± 2	200	Loss of nuclei
			8	2,500	3	20 ± 2	200	None
			9	625	3	20 ± 2	200	None
			10	625	3	20 ± 2	200	None
			11†	5,000	20	20 ± 2	200	None
			12	5,000	20	20 ± 2	200	Loss of nuclei
			13	2,500	20	20 ± 2	200	Loss of nuclei
			14	2,500	20	20 ± 2	200	Loss of nuclei
			15	625	20	20 ± 2	200	None
			17	625	20	20 ± 2	200	None
			18	312	20	20 ± 2	200	None
			19	312	20	20 ± 2	200	None
MRT 4	7 mm	42 μm	5	10,000	20	42 ± 4	200	Tissue necrosis
			6	10,000	20	42 ± 4	200	Tissue necrosis
			7	2,500	20	42 ± 4	200	Loss of nuclei
			8	2,500	20	42 ± 4	200	Loss of nuclei
MRT 5	37 μm	4 mm	9	1,250/312	21	37 ± 3	200	Loss of nuclei/none
			10	1,250/312	21	37 ± 3	75	None/none
			11	1,250/312	21	37 ± 3	75	None/none
			12	1,250/625	21	37 ± 3	200	None/none
			13	1,250/625	21	37 ± 3	200	None/none
			14	1,250/625	21	37 ± 3	75	None/none
			15	1,250/625	21	37 ± 3	75	Loss of nuclei/none
			16	2,500/312	21	37 ± 3	200	None/none
			17	2,500/312	21	37 ± 3	200	Loss of nuclei/none
			18	2,500/312	21	37 ± 3	75	None/none
			19	2,500/312	21	37 ± 3	75	None/none
			20	2,500/625	21	37 ± 3	200	None/none
			21	2,500/625	21	37 ± 3	200	None/none
			22	2,500/625	21	37 ± 3	75	Loss of nuclei/none
			23	2,500/625	21	37 ± 3	75	Loss of nuclei/none
			24	1,250/312	21	37 ± 3	200	None/none

正常組織への影響

Slatkin et al, Proc. NAS USA 92, 8783, 1995

9L Rat Gliosarcoma

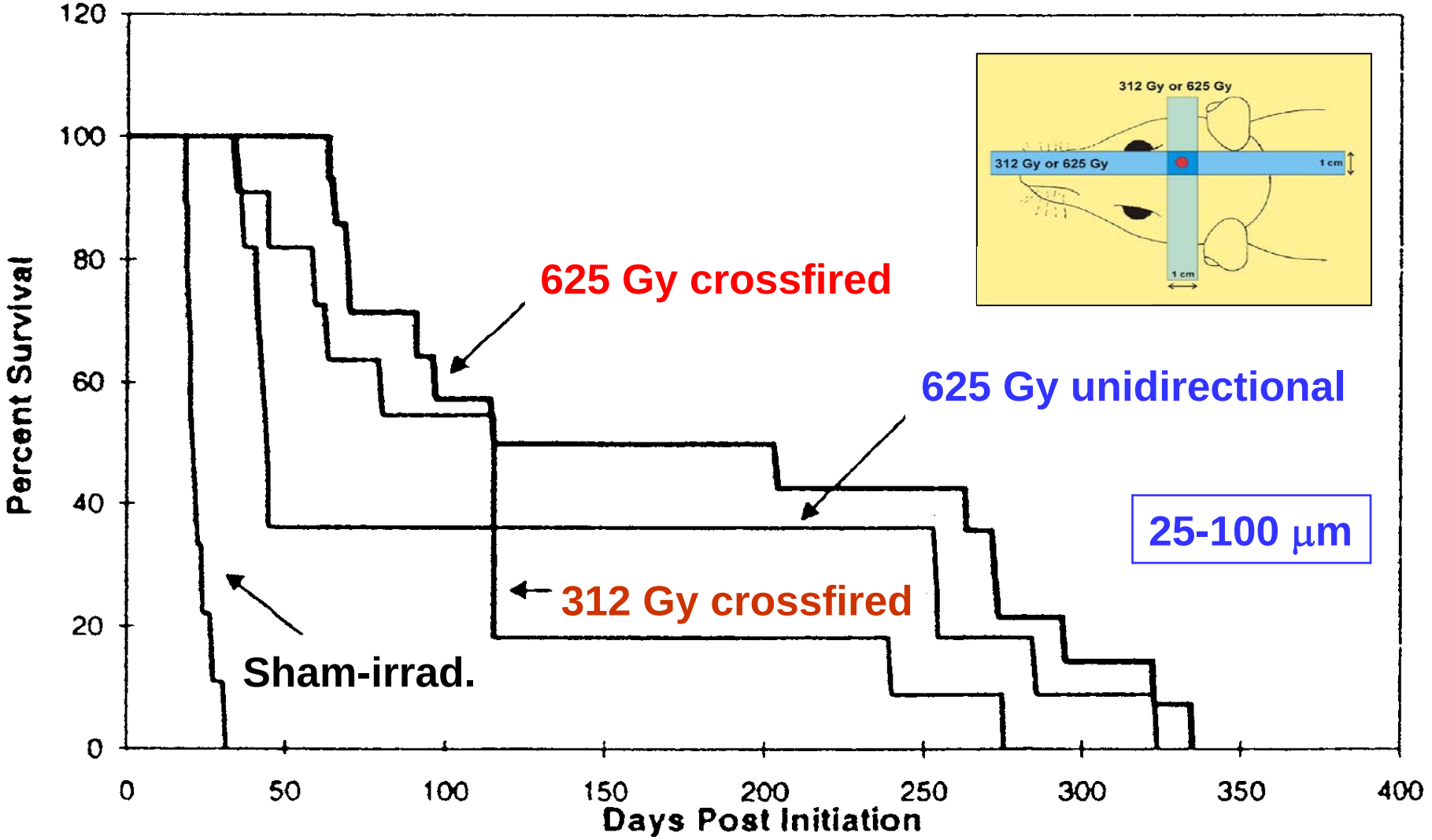

Laissue et al, Int. J. Cancer 78, 654, 1998

Murine EMT-6 carcinoma

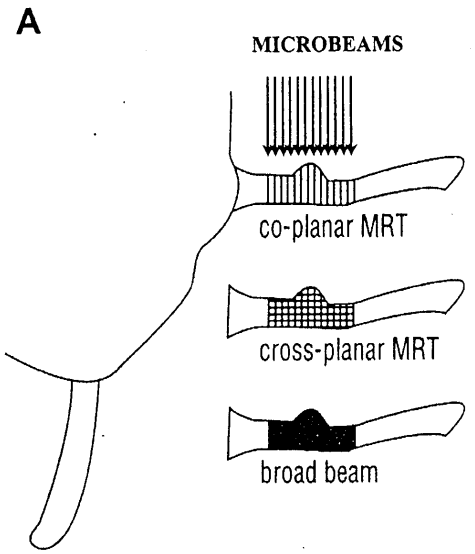

90-300 μm

ED_{50}/TCP_{50}

Comparison for the Three ... or Tumor Ablation and
ED_{50} for Failure of Nearly ... d by Probit Analysis of
the E ... se

Irradiation geometry	TCP_{50} (int dose,	Therapeutic index: ED_{50} for failure of nearly complete hair regrowth/ TCP_{50}
Co-planar microbeams	403 ±	1.33 ± 0.07
Cross-planar microbeams	277 ±	1.51 ± 1.0
Broad beams	37.1 ±	0.79 ± 0.03

1.33 ± 0.07

1.51 ± 1.0

0.79 ± 0.03

Dilmanian et al, Radiat. Res. 159, 632, 2003

9L Rat Gliosarcoma

腫瘍位置でのピーク線量と谷線量

Configuration, no. of rats, and category	Beam spacing center to center (μm)	In-slice skin-entrance dose (Gy)	In-slice dose at center of brain (Gy)	Valley dose at center of brain, averaged laterally (Gy)
A (n = 5) High dose	50	150	108	20
B (n = 5) High dose	50	250	179	34
C (n = 5) High dose	50	300	215	40
D (n = 5) Tolerable dose	75	250	179	17
E (n = 6) High dose	75	300	215	20
F (n = 6) High dose	75	500	359	33
G (n = 3) Tolerable dose	100	500	359	19
Unirradiated controls (n = 17)	N/A	N/A	0	0
Broad beams Joel et al., 1990 (n = 16)	N/A	N/A	22.5	N/A

ビーム幅：27 μm

Dilmanian et al, Neuro-Oncol. 4, 26, 2002

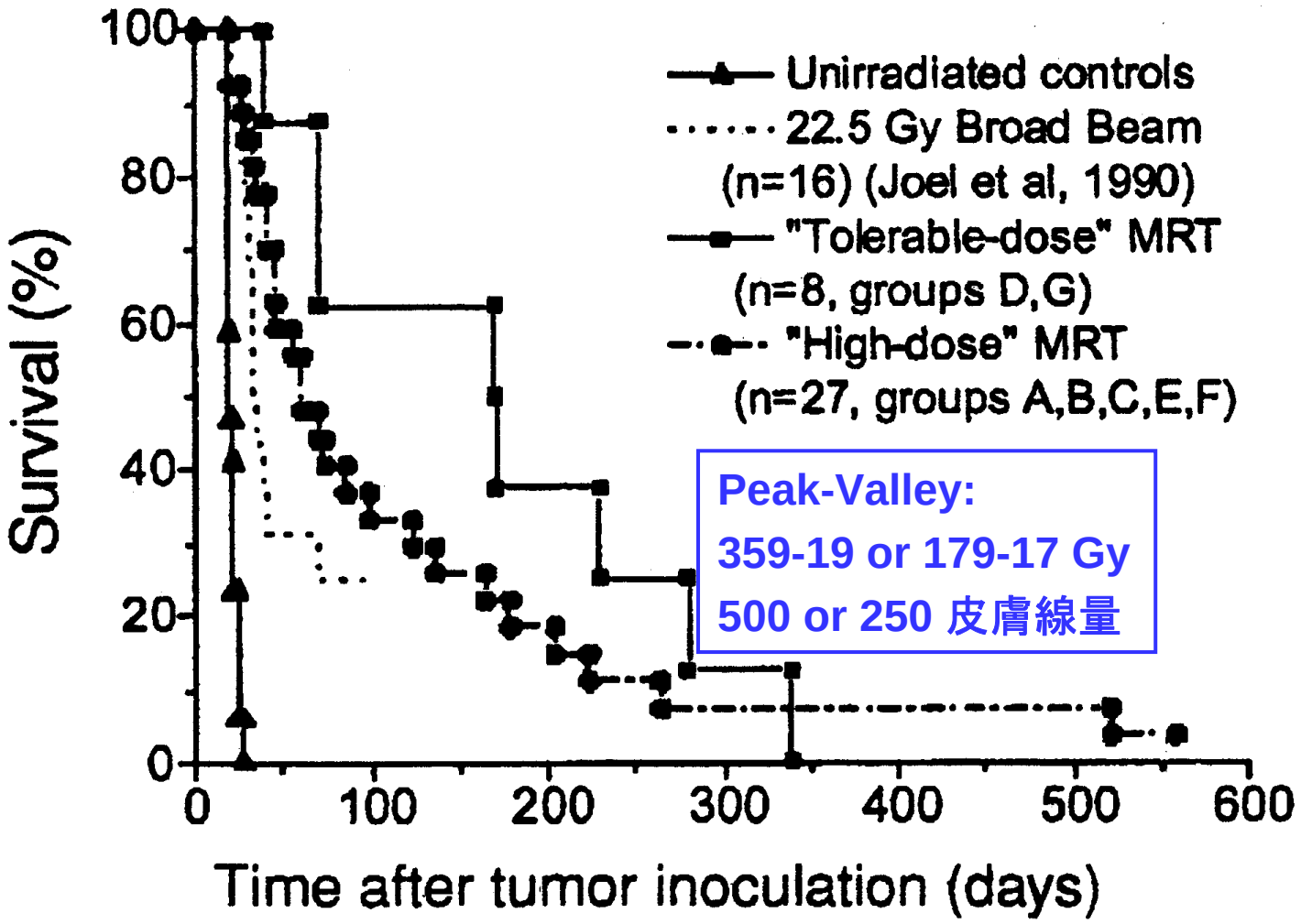

Fig. 3. Survival curves of rats receiving tolerable and high-dose MRT, the unirradiated controls, and the broad beams from Joel et al. (1990).

Dilmanian et al, Neuro-Oncol. 4, 26, 2002

文献情報

	発表年	2006	2007	2008	2009	2010	2011/12	計
生物影響	組織反応	1	1	3	0	2	2	9
	治療効果	2	0	3	2	1	1	9
治療設計･線量計測他		1	2	4	6	4	4	21
概説･総説		0	1	1	0	3	0	5
計		4	4	11	8	10	7	44

（1）正常組織への損傷は、broad beam の場合よりも小さい

（2）minibeamよりもmicrobeamのほうが効果的

（3）増感剤（Gd）の併用が効果的

（4）損傷の腫瘍選択性が高い（血管への作用）

（5）照射法の提案

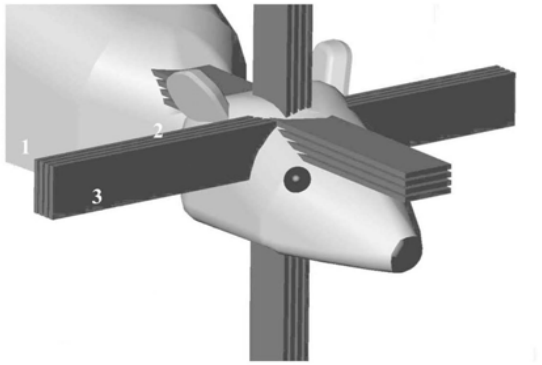

(*a*)

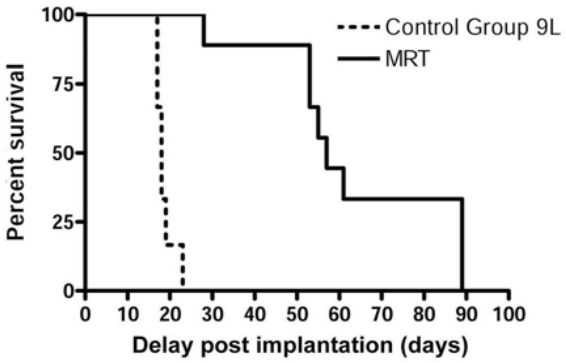

(*b*)

Figure 1

(*a*) Schematic representation of the irradiation geometry. The three arrays, administered at intervals of 24 h, produce a composite irradiation volume in the brain of 10.4 × 10.4 × 14.6 mm at the tumor site. (*b*) Survival curves of untreated (dashed line) and treated (solid line) Fisher rats bearing an intra-cerebral 9 L gliosarcoma.

Serduc et al, J. Synchrotron Radiat. 16, 587-590, 2009

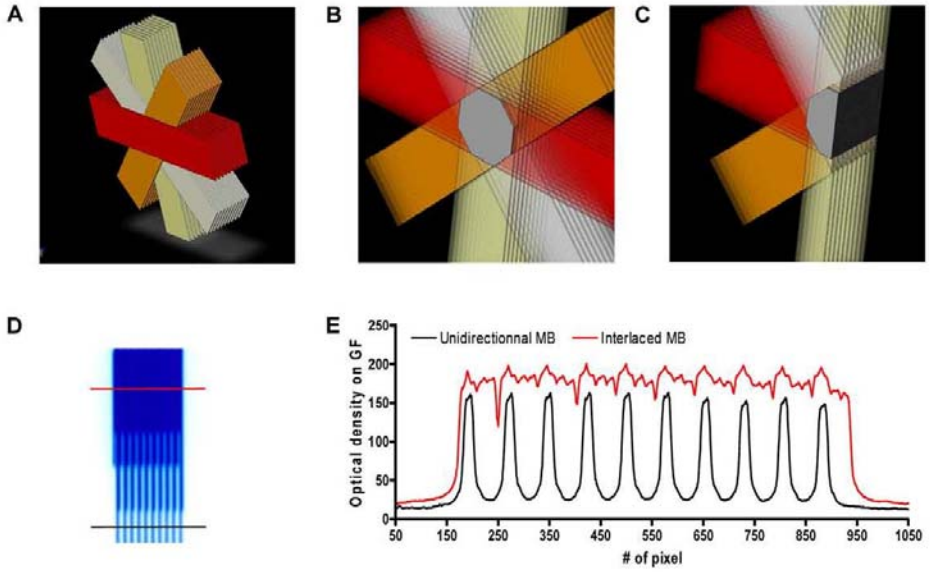

Figure 1. Schematic representation of the irradiation geometry in normal rats. (A–C). Four arrays of 10 MBs (50 μm wide, 200 μm on-center distance) were interlaced and created a 2×2×2.2 mm^3 target region where the radiation dose is homogenous. D- Gafchromic® film image of interlaced MBs; the upper part corresponds to a centre-to-centre distance of 200 μm. The radiation target corresponds to the region where all the 4 arrays of MBs interlaced. E- Dose profiles measured on the Gafchromic® film shown in (D). The red line shows the dose in the interlaced region. The dose profile produced in the spatially fractionated irradiation and which is delivered by a single array of MBs is shown with the black line.
doi:10.1371/journal.pone.0009028.g001

Serduc et al, PLOS ONE, 5(2), e9028, 2009

MRT効果を決めるパラメータは？

＊ピーク線量と谷線量の関係は？

＊その作用機構は？

腫瘍血管への選択的損傷？

a. Bouchet et al, Int. J. Radiat. Oncol. Biol. Phys. 78, 1503, 2010.

b. Sabatasso et al, ibid. 80, 1522, 2011.（未成熟血管の損傷大）

（cf. 正常血管の損傷を検出せず：Serduc et al, ibid. 64, 1519, 2006）

＊ビーム幅、ビーム間隔の設定基準は？

＊ピーク線量の設定基準は？

＊ 治療への具体的な方法は？

短時間照射！　10000 Gy/sec?

最適エネルギーは？